Imaging the Lipidome: ω-Alkynyl Fatty Acids for Detection and Cellular Visualization of Lipid-Modified Proteins

Rami N. Hannoush* and Natalia Arenas-Ramirez

Department of Protein Engineering, Genentech, Inc., 1 DNA Way, South San Francisco, California 94080

Fatty acylation of cellular proteins is vital, controlling protein−protein and protein−membrane interactions. Protein fatty acylation is the covalent attachment of lipids onto proteins. This serves to modulate the proteins' physicochemical properties and biological functions and to direct their targeting for activation within cells. As such, protein fatty acylation regulates intracellular protein trafficking and sorting, signal transduction pathways, and homeostasis (1−3).

Several classes of protein fatty acylation exist in eukaryotes. These primarily include N-myristoylation and S-palmitoylation (Figure 1, panel a). Typically, N-myristoylated proteins contain the saturated 14-carbon myristate group bound to an exposed N-terminal glycine residue through a stable amide bond. S-Palmitoylation on the other hand comprises the reversible addition of a 16-carbon palmitate or longer fatty acid chains onto cysteine residues *via* a labile thioester linkage. While S-palmitoylation is dominant in living cells, N-palmitoylation has been observed in Hedgehog and Spitz secreted proteins (4, 5) and presumably occurs through migration of the palmitoyl group on a cysteine to form the amide linkage.

Despite the critical role of protein fatty acylation in physiology, few methods exist that are highly sensitive for detecting lipid-modified proteins (6, 7). Traditional methods involve metabolic labeling with radioactive fatty acids (8), but they are time-consuming as they require long autoradiographic exposure time, not to mention the hazards of handling radioisotopes. Recently, pioneering work described the metabolic incorporation of fatty acid analogues bearing an azido group and their use to detect fatty acylated proteins by a Staudinger ligation reaction (9−12). This approach was used for labeling recombinant proteins in bacteria (13) and for

ABSTRACT Fatty acylation or lipid modification of proteins controls their cellular activation and diverse roles in physiology. It mediates protein−protein and protein−membrane interactions and plays an important role in regulating cellular signaling pathways. Currently, there is need for visualizing lipid modifications of proteins in cells. Herein we report novel chemical probes based on ω-alkynyl fatty acids for biochemical detection and cellular imaging of lipid-modified proteins. Our study shows that ω-alkynyl fatty acids of varying chain length are metabolically incorporated onto cellular proteins. Using fluorescence imaging, we describe the subcellular distribution of lipid-modified proteins across a panel of different mammalian cell lines and during cell division. Our results demonstrate that this methodology is a useful diagnostic tool for analyzing the lipid content of cellular proteins and for studying the dynamic behavior of lipid-modified proteins in various disease or physiological states.
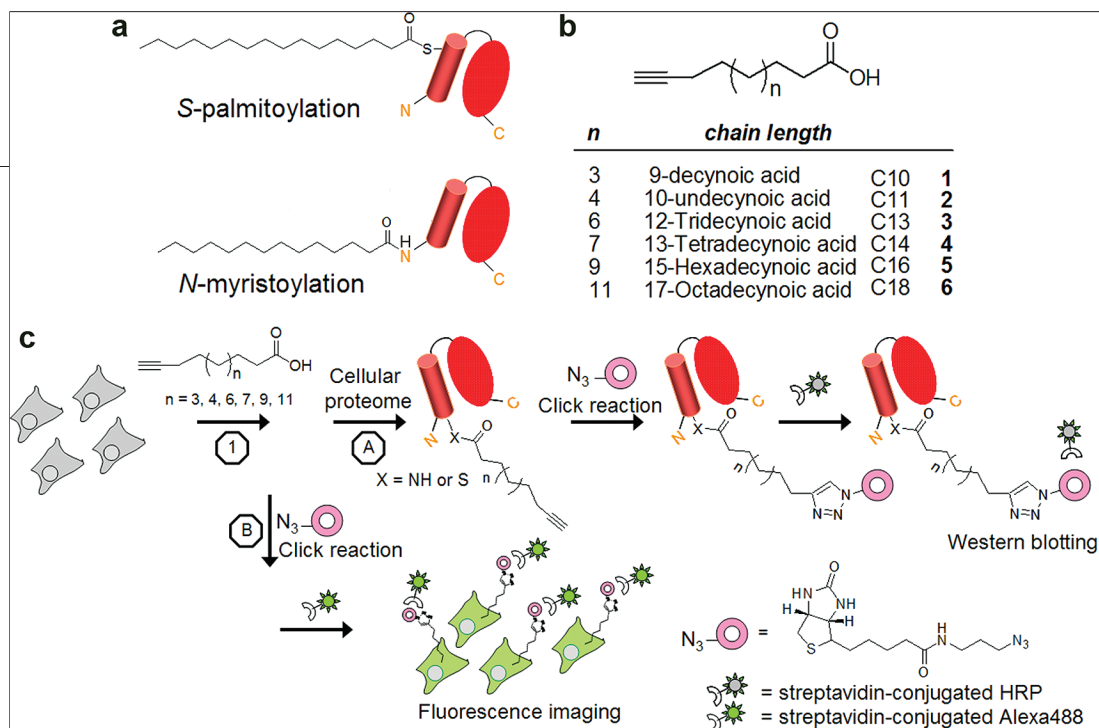
*Corresponding author,
hannoush.rami@gene.com.

Figure 1. Labeling and imaging of cellular proteins with bioorthogonal ω-alkynyl fatty acids. a) Chemical structures of *N*-myristate and *S*-palmitate groups covalently attached to proteins. **b)** ω-Alkynyl fatty acid analogues used in this study. **c)** Process for labeling cellular lipid-modified proteins with fatty acid analogues. Synthetic ω-alkynyl fatty acids are added to cultured cells and metabolically incorporated into acylated proteins. After workup, the alkynyl group is chemoselectively ligated to azide-tagged biotin or fluorophore by a Cu^1-catalyzed alkyne-azide [3 + 2] cycloaddition reaction. The conjugated proteins are separated by gel electrophoresis and detected by streptavidin-linked horseradish peroxidase (route A) or alternatively detected by streptavidin-Alexa488 and imaged using fluorescence microscopy (route B).

identifying fatty acylated proteins that are localized in mitochondria or posttranslationally modified during apoptosis (*10, 11*). However, all of these studies stopped short of characterizing the subcellular distribution of lipid-modified proteins. Hence, there is still need for alternative methods aimed at visualizing protein fatty acylation in cells, as this has not been addressed. Here we report the synthesis and investigation of a suite of nonradioactive fatty acids containing alkyne groups, their metabolic incorporation onto cellular proteins, and their utility as tool reagents for detecting and visualizing lipid-modified proteins in cultured cells (Figure 1, panels b and c).

RESULTS AND DISCUSSION

Design and Synthesis of ω-Alkynyl Fatty Acids. In this study, we describe the subcellular distribution of lipid-modified proteins by using alkynyl fatty acids. We chose to use alkyne groups because they maintain the hydrophobicity of the fatty acid carbon chain and hence minimize changes in the physicochemical properties of fatty acids and their interactions with lipids and because they are metabolically inert but sufficiently reactive under appropriate conditions. Indeed, the chemical properties of alkynes have been recently exploited in the

study of glycoconjugates (*14*) and activity-based protein profiling (*15, 16*).

We introduced alkyne groups at the ω-position (terminal end that is farthest from the carboxyl functionality) of fatty acids (Figure 1, panel b) because previous work demonstrated that the biosynthetic enzymes that incorporate fatty acids onto proteins are tolerant to modifications at this terminal position (*17, 18*). Our ω-alkynyl myristate and palmitate analogues were synthesized from the corresponding alcohols containing internal alkynes *via* a zipper reaction (*19*) that allows isomerization of an internal alkyne to a terminal alkyne (see Supplementary Scheme 1). This was followed by Jones oxidation to yield the ω-alkynyl myristate and palmitate analogues in high yield and purity.

Biochemical Incorporation of ω-Alkynyl Fatty Acids onto Cellular Proteins. First, we wished to demonstrate that the synthetic fatty acid analogues were metabolically incorporated onto cellular proteins. To do so, ω-alkynyl fatty acids with 10 (**1**), 11 (**2**), 13 (**3**), 14 (**4**), 16 (**5**), and 18 (**6**) carbon atoms (Figure 1, panel b) were added to cultured MDCK epithelial cells and incubated for 24 h. After preparing the cellular proteome, the alkynyl group incorporated onto acylated proteins was chemoselectively ligated to azide-tagged biotin (for synthesis, see Supplementary Scheme 2) or fluorophore by a

Cu[1]-catalyzed alkyne-azide [3 + 2] cycloaddition reaction (20) (Figure 1, panel c). The conjugated proteins were separated by gel electrophoresis and analyzed by Western blot using streptavidin-linked horseradish peroxidase (Figure 2, panel a). Samples treated with ω-alkynyl fatty acids showed significant labeling relative to untreated control. The degree of labeling was dependent on the carbon chain length, indicative of the specific nature of the bioorthogonal labeling procedure with ω-alkynyl fatty acids. We ascribe the background bands detected in the untreated DMSO control to endogenously biotinylated proteins considering that bioorthogonal click chemistry exhibits specific labeling under these conditions (see Supplementary Figure 1) (14−16). The C13, C14, and C16 probes exhibited the highest degree of protein incorporation. This is a reasonable expectation considering that the majority of known protein lipid modifications in cells comprise myristoylation and palmitoylation. Importantly, ω-alkynyl fatty acids were taken up and metabolically incorporated into other cell lines such as RAW2647 macrophages and mouse L-cells (see Supplementary Figure 2), demonstrating the versatility of these probes. It is worth noting that differences in labeling among the individual ω-alkynyl fatty acids indicate they target diverse sets of proteins.

To demonstrate the specificity of metabolic incorporation, we analyzed the type of chemical linkage via which ω-alkynyl fatty acid probes attach onto proteins. We treated alkyne-labeled proteins from MDCK cells with hydroxylamine, which specifically removes fatty acids attached via thioester linkages but not amide bonds (6) (Figure 2, panel b). The C16 ω-alkynyl fatty acid showed substantial sensitivity to hydroxylamine treatment, suggesting that it is predominantly attached via thioester linkages and hence labels S-palmitoylated proteins. On the other hand, the 13- and 14-carbon fatty acid chains predominantly incorporated via amide bonds due to their relative resistance to hydroxylamine treatment. Collectively, these experiments validate the utility of C14 and C16 ω-alkynyl fatty acids as probes for protein N-myristoylation and S-palmitoylation, respectively. They also demonstrate that C10, C11, and C18 predominantly attach via thioester bonds (Figure 2, panel b), and hence serve as probes of S-acylation as well. The interesting finding about C10 and C11 adds to the toolbox of fatty acid probes of S-acylation and is consistent with prior examples illustrating the attachment
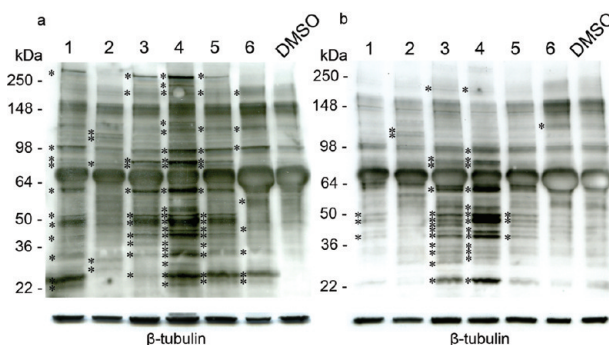

Figure 2. Biochemical detection of lipid-modified proteins. a) MDCK cells were treated with ω-alkynyl fatty acid probes (100 μM) as indicated for 24 h. Lane 1: C10, lane 2: C11, lane 3: C13, lane 4: C14, lane 5: C16, lane 6: C18. DMSO lane represents lysates treated with DMSO instead of fatty acids and processed in the same manner as the fatty-acid-treated lysates. Cellular proteins were isolated, reacted with biotin-azide, resolved by gel electrophoresis, and detected by Western blotting with streptavidin-HRP, as described in Methods. Asterisks denote bands labeled by treatment with probe, as judged visually by appearance of new bands relative to untreated DMSO control. b) In parallel, membranes were treated with 5% hydroxylamine for 72 h before detection with streptavidin-HRP.

of decanoic acid to acyl carrier proteins via a thioester linkage (21).

The ω-alkynyl fatty acids were metabolically incorporated onto cellular proteins in a time- and dose-dependent manner, indicating that labeling with ω-alkynyl fatty acids is dependent on active cellular metabolism. Treatment of MDCK cells with C14, C16, or C18 results in labeled protein bands that are observed within 1 h and that exhibit a time-dependent increase in their intensity over a 6 h time period (see Supplementary Figure 3). In a similar fashion, treatment with increasing concentration of C14, C16, or C18 shows dose-dependent metabolic incorporation at 4 h (see Supplementary Figure 4). Because protein N-myristoylation is a co-translational event, we show that treatment with the protein synthesis inhibitor cycloheximide inhibits protein labeling with C14 (see Supplementary Figure 5, panel a). Furthermore, competition experiments with myristic and palmitic acids demonstrate that the ω-alkynyl C14 and C16 fatty acids serve as specific probes for protein N-myristoylation and S-palmitoylation in cells, respectively (see Supplementary Figure 5, panels b and c). Together, these results illustrate that ω-alkynyl fatty acids are sufficiently taken up and well
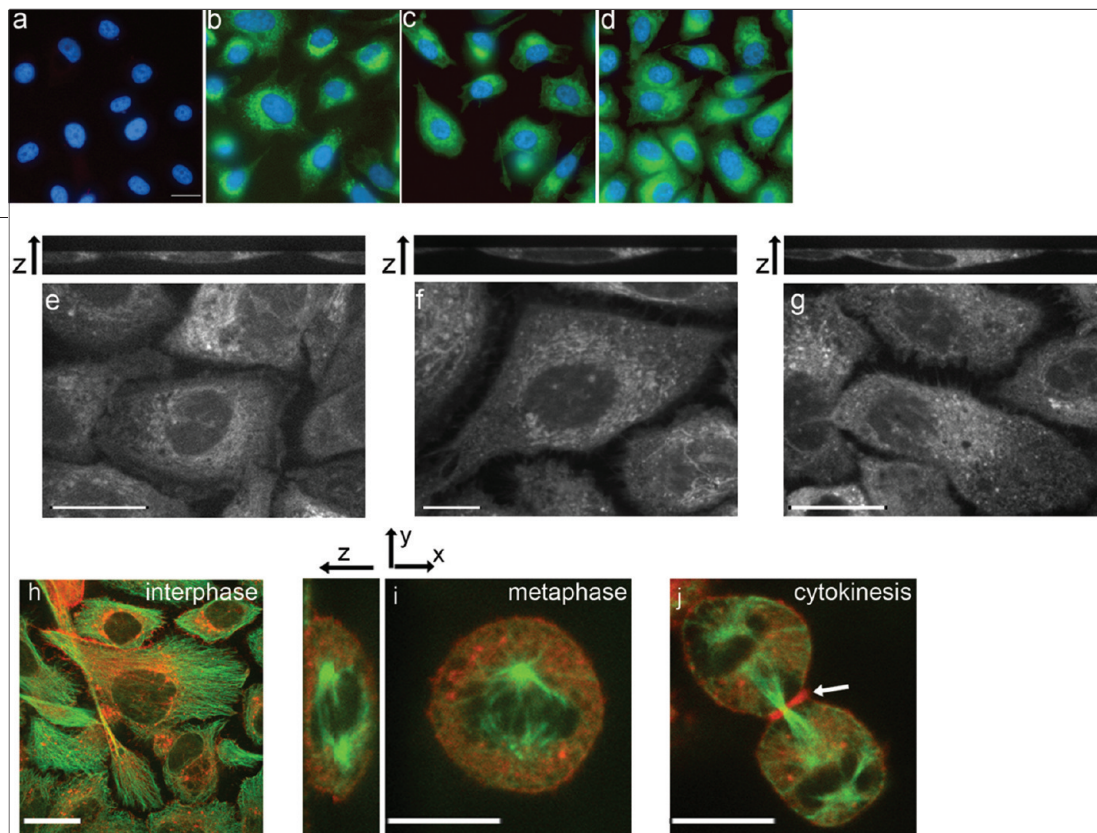
Figure 3. Cellular imaging of lipid-modified proteins. a−d) Fluorescence microscopy of PC3 cells not labeled in the absence (a) or labeled in the presence of ω-alkynyl fatty acids C14 (b), C16 (c), and C18 (d). Cells were treated with DMSO or ω-alkynyl fatty acids (100 μM) as indicated for 3 h. Cells were then fixed, permeabilized, reacted with rhodamine-azide (shown in green), and imaged by epifluorescence microscopy using a 40x objective. e−g) Confocal section of PC3 cells treated with C14 (e), C16 (f), and C18 (g). Cells were treated as in panels a−d and imaged by confocal microscopy using a 63x oil objective. All images were acquired the same way. The fluorescence along the *z*-axis is shown on top of each confocal section. h−j) Confocal section of PC3 cells in interphase (h), metaphase (i), and cytokinesis (j), treated with C16 (red) and stained with tubulin (green). Cells were treated as in panels a−d except that they were fixed in methanol and imaged by confocal microscopy using a 63x oil objective. All images were acquired the same way. The fluorescence along the *z*-axis is shown on the left-hand side of panel i. Arrow in panel j indicates cleavage furrow where palmitoylated proteins concentrate. Scale bar = 10 μm.

tolerated by cultured cells, readily recognized by the biosynthetic machinery, and efficiently incorporated onto cellular proteins.

Imaging of Lipid-Modified Cellular Proteins. To demonstrate the broad utility of ω-alkynyl fatty acids, we performed fluorescence microscopy to visualize cellular fatty acylated proteins. Cells were treated with vehicle or the various ω-alkynyl fatty acid analogues, extensively washed to remove excess probe, and then fixed. To differentiate labeled proteins from possible incorporation of probes into cellular phospholipids, cells were either methanol fixed or fixed with paraformaldehyde followed by treatment with detergent to remove lipids. Cells were then processed for the click reaction with rhodamine azide or biotin azide followed by streptavidin-conjugated Alexa488. A high fluorescence signal was observed in samples treated with ω-alkynyl fatty acids compared to a minimal signal in DMSO-treated samples in prostate cancer PC3 cells (Figure 3, panels a−d and Supplementary Figure 6), mouse fibroblast L-cells (Supplementary Figure 7) and RAW2647 macrophages

(Supplementary Figure 8). The signal-to-background ratio was significantly higher in samples processed with rhodamine azide compared to biotin azide; this is mainly due to endogenously biotinylated proteins that contribute to background and is also consistent with background observed in streptavidin biochemical detection (Supplementary Figure 1). Hence, rhodamine-azide was used in fluorescence microscopy experiments for detection of lipid-modified proteins. Fluorescence images show different subcellular distributions of proteins labeled with the various ω-alkynyl fatty acids. Interestingly, cellular C14-, C16-, and C18-labeled proteins are distributed in a punctate pattern outside the nucleus, localize to a varying degree in vesicular structures in the cytoplasm. and label the plasma membrane and membrane ruffles (Figure 3, panels e−g and see Supplementary movies 1, 2, and 3), consistent with membrane targeting of lipid-modified proteins. There are also subtle differences in the fluorescence localization between C14, C16, and C18 (see Supplementary movies 1, 2, and 3 and Supplementary Figure 9), with C14 and C16

labeling dense objects around the nucleus and C18 labeling fluorescent objects that are more dispersed throughout the cytoplasm. Furthermore, based on our cellular images, it is likely that some labeled lipid-modified proteins may in part be localized in mitochondria, among other organelles. It remains to be determined which cellular compartments are occupied by lipid-modified proteins and how this depends on the specific type of ω-alkynyl fatty acid used. Nevertheless, this set of data is to our knowledge the first cellular view of global lipid-modified proteins.

Next, we demonstrated that ω-alkynyl fatty acids can be used to analyze the distribution of lipid-modified proteins in different cellular states. As a test case, we monitored PC3 cells that are undergoing cell division and have been labeled with C16 ω-alkynyl fatty acid in addition to a tubulin marker (Figure 3, panels h−j and Supplementary movies 4 and 5). Metaphase cells show a distinct distribution of C16-labeled proteins at the plasma membrane and in dense structures around the spindle and throughout the cell body (Figure 3, panel i and Supplementary movie 4). Interestingly, during cytokinesis, C16-labeled proteins concentrate at the cleavage furrow, the site of cell division (see arrow, Figure 3, panel j and Supplementary movie 5). While the biological significance of this observation is out of the scope of this paper, these experiments shed light on the behavior of S-palmitoylated proteins during cell division and highlight the potential application of our probes in different cellular contexts.

Monitoring Turnover of Lipid-Modified Cellular Proteins. We then decided to examine the turnover of lipid-modified proteins in cells to gain insight into their dynamic behavior. In this regard, we performed a pulse-washout experiment as follows: PC3 cells were pulse labeled with C16 ω-alkynyl fatty acid for 3 h, washed extensively then incubated in growth medium without C16 and subsequently fixed at various time points (Figure 4, panel a). We observe that C16-labeled proteins undergo rapid turnover as noted by the loss in fluorescence signal within 3−6 h (Figure 4, panels b and c). It will be interesting to determine in the future how the turnover of lipid-modified proteins is affected under different conditions and how it varies with the individual labeling probes. Nevertheless, these experiments shed light onto the turnover of S-palmitoylated proteins in
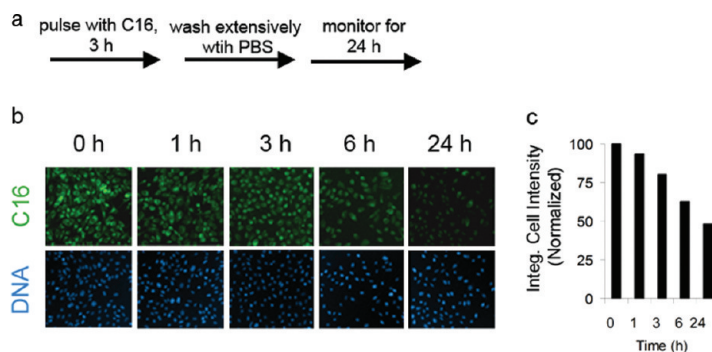

Figure 4. Monitoring turnover of lipid-modified proteins. a) Schematic of the pulse-washout experiment. PC3 cells were pulsed with C16 (100 μM) for 3 h, washed extensively with PBS, and allowed to grow in full media before being fixed at various time points. Samples were then processed for click reaction with rhodamine azide and visualized by epifluorescence microscopy. b) Fluorescent images showing the decay in signal of C16-labeled proteins (green) at the indicated time points (1, 3, 6, 24 h time points) immediately after washout of the C16 probe (0 h time point). Nuclei are shown in blue and are used as a control for cell number. Images were captured by using a 10x air objective. c) Quantification of the normalized integrated cell intensity (%) in images from (b). A total of ~5000 cells per time point were scored by MetaXpress imaging algorithm.

cells and provide evidence that ω-alkynyl probes should aide in monitoring the dynamics of lipid-modified proteins in various cellular states.

Conclusion. In summary, we developed sensitive, nonradioactive chemical probes for biochemical detection and cellular imaging of protein fatty acylation. We also described a simple and efficient way to synthesize ω-alkynyl myristic and palmitic acid probes *via* a zipper reaction and biochemically validated C10, C11, C13, C14, C16 and C18 probes in different mammalian cell lines and characterized their distribution by fluorescence imaging. Previous studies utilizing azido fatty acids (9−11) and a C18-alkyne probe (22) were aimed at biochemical detection of fatty acylation but stopped short of characterizing the subcellular distribution of lipid-modified proteins. This study's fluorescence imaging of cellular lipid-modified proteins across a diverse panel of cell lines, turnover of C16-labeled proteins, and the finding that S-palmitoylated proteins concentrate at the cleavage furrow during cell division demonstrate that this methodology will be useful for probing the dynamics of lipid-modified proteins.

Because the probes reported herein are easy to handle, we anticipate that they will serve as an alternative to radioactively labeled fatty acids and their lengthy

and hazardous experimental protocols. Furthermore, they pave the way into global lipidomic analysis of cellular acylated proteins (22) and may find usage in biological studies of novel myristoylated proteins (11, 23, 24). We believe that incorporation of an alkyne tag would offer advantages in labeling lipid-modified proteins compared to azide tags because they maintain the hydrophobicity of the carbon chain and minimize interference with the hydrophobic lipid environment. Indeed, while this manuscript was under review, Hang and co-workers described C14, C16, and C18 as more efficient probes for labeling lipid-modified proteins compared to their azido counterparts (25). These probes along with C10, C11, and C13 probes described herein comprise a novel chemical toolbox for visualizing lipid-modified proteins during various physiological states of the cell or for further proteomic analysis of lipid-modified proteins. A future development of this methodology would be to investigate the identity of proteins detected by the individual probes and to understand the factors governing their selectivity in a cellular context. We are currently extending this methodology in our laboratory to label and follow the dynamic behavior of specific proteins in response to different stimuli. The simplicity of our method and the specificity of metabolic incorporation of ω-alkynyl fatty acids make them ideal probes to study post-translational lipid modifications of cellular proteins.

METHODS

Cell Culture. Raw 264.7 macrophages (ATCC no. CCL-2278) were grown in high glucose Dulbecco's Modified Eagle's Medium (DMEM) supplemented with 10% fetal bovine serum (FBS) and glutamax (2 mM). MDCK (canine kidney epithelial cells, ATCC no. CCL-34) were grown in DMEM media supplemented with 10% FBS. PC-3 cells (ATCC no. CRL-1435) were grown in F-12K Medium supplemented with 10% FBS. Mouse L-cells (ATCC no. CRL-2648) were cultured in DMEM media supplemented with 10% FBS. All cells used were incubated in a 5% CO_2 humidified chamber at 37 °C for 24 h before any experiment.

Labeling and Detection of Lipid-Modified Proteins in Cell Extracts. The ω-alkynyl fatty acid analogues were dissolved in DMSO to generate 50 mM stock solutions and were stored at −80 °C. Before cell treatment, the analogues were dissolved in DMEM serum-free media supplemented with 5% BSA (fatty-acid-free) at a final concentration of 100 μM. The fatty acid−media solutions were sonicated for 15 min at RT and then allowed to precomplex for 15 min at RT.

Cells were seeded with complete media onto 6-well plates (8×10^5 cells/well) and incubated for 24 h before treatment. After the growth media was removed, cells were washed once with PBS before adding 2 mL of the ω-alkynyl fatty acid containing media. After a 24 h incubation period at 37 °C/5% CO_2, cells were washed three times with cold PBS, and cell extracts were prepared in 400 μL of lysis buffer (1% Nonidet P-40/150 mM NaCl/Pierce protease and phosphatase inhibitor cocktail/100 mM sodium phosphate, pH 7.5). To obtain a final proteome concentration of 2 mg mL^{-1} (protein concentration determined by BCA kit), cell lysates were concentrated by centrifugation for 15 min at 14,000 rpm at 4 °C with Nanocep centrifugal ultrafiltration devices. Protein extracts (~45 μg) were then subjected to the probe labeling reaction in a 25 μL volume, for 1 h at RT, at final concentrations of the following reagents (14, 16): 0.1 mM biotin-azide, 1 mM Tris(2-carboxyethyl)phosphine hydrochloride (TCEP, Sigma-Aldrich) dissolved in water, 0.2 mM Tris[(1-benzyl-1H-1,2,3-triazol-4-yl)methyl]amine (TBTA, Sigma-Aldrich) dissolved in DMSO/tert-butanol (20%/80%) and 1 mM $CuSO_4$ in PBS. The order of addition of the reagents to the protein extracts is important for the reaction and has to be followed as described above.

Western Blotting. Labeled protein lysates were resolved by SDS−PAGE using 4−20% Tris-glycine gels. For immunoblotting of biotin-labeled proteins after electrophoresis, proteins were transferred onto a nitrocellulose membrane, which was blocked with PBS, 0.1% Tween-20 [PBST], and 5% nonfat dried milk for 2 h at RT or overnight at 4 °C. The membrane was washed three times with PBST (5 min each) and incubated with streptavidin-horseradish peroxidase (Zymed, 1:1250 in PBST) for 1 h at RT. The membrane was washed with PBST three times (10 min each) and developed using enhanced chemiluminescence reagent according to manufacturer's recommendation (Amersham Biosciences). For the hydroxylamine-sensitivity assay, following the transfer of proteins to nitrocellulose membranes, the membranes were incubated 65−72 h at RT with PBST and 5% NH_2OH (Sigma-Aldrich). After hydroxylamine treatment, membranes were blocked with 5% nonfat dried milk in PBST for 2 h at RT or overnight at 4 °C and analyzed by streptavidin blot as described above. To demonstrate equal levels of protein loading, streptavidin blots were stripped with Pierce stripping buffer for 15 min at RT and reprobed with an anti-β-tubulin HRP antibody and developed with enhanced chemiluminescence reagent.

Fluorescence Microscopy. Cells were seeded onto 12-well plates (4×10^5 cells $well^{-1}$) containing glass coverslips and incubated for 24 h before treatment. The growth medium was removed, and cells were washed once with PBS before adding 1 mL of medium containing the ω-alkynyl fatty acid at the indicated concentration. After 24−48 h incubation at 37 °C/5% CO_2, cells were washed three times with PBS to remove excess probe and fixed with 4% paraformaldehyde (PFA) for 10 min at RT. Cells were then permeabilized with PBS/0.1% triton X-100 for 1−2 min at RT, washed extensively with PBS, and subjected to the click reaction in a 50 μL volume at final concentrations of the following reagents: 0.1 mM biotin-azide or rhodamine-azide, 1 mM TCEP dissolved in water, and 1 mM $CuSO_4$ in PBS at RT for 1 h. The labeled cells were rinsed extensively with PBS and blocked in PBS/5% BSA for 45 min at RT. Cells were stained with streptavidin-conjugated AlexaFluor 488 (Invitrogen cat. no. S32354, 1:500) in PBS/5% BSA for 45 min at RT, and nuclei were stained with Hoechst 33342 (MP no. H21492; 1:10,000 in PBS) for 10 min at RT. For labeling with rhodamine-azide, cells were directly stained with Hoechst. For tubulin staining, cells were fixed in precooled methanol at −20 °C for 5−10 min and processed for the click reaction as described above followed by staining with antitubulin antibody and the appropriate secondary Alexa488 conjugate antibody. Fluorescent images were captured on an inverted Zeiss AX10 microscope equipped with a

CoolSnap CCD camera (Roper Scientific), and images were analyzed with Slidebook 4.1 software (Intelligent Imaging Innovation). Z-Sections were acquired with 0.3 μm spacing. On average, 50−70 z-sections were acquired per image.

Supporting Information Available: This material is available free of charge *via* the Internet.

REFERENCES

1. Resh, M. D. (2006) Trafficking and signaling by fatty-acylated and prenylated proteins, *Nat. Chem. Biol. 2*, 584−590.
2. Greaves, J., and Chamberlain, L. H. (2007) Palmitoylation dependent protein sorting, *J. Cell Biol. 176*, 249−254.
3. Zhang, F. L., and Casey, P. J. (1996) Protein prenylation: molecular mechanisms and functional consequences, *Annu. Rev. Biochem. 65*, 241−270.
4. Pepinsky, R. B., Zeng, C., Wen, D., Rayhorn, P., Baker, D. P., Williams, K. P., Bixler, S. A., Ambrose, C. M., Garber, E. A., Miatkowski, K., Taylor, F. R., Wang, E. A., and Galdes, A. (1998) Identification of a palmitic acid-modified form of human Sonic hedgehog, *J. Biol. Chem. 273*, 14037−14045.
5. Miura, G. I., Buglino, J., Alvarado, D., Lemmon, M. A., Resh, M. D., and Treisman, J. E. (2006) Palmitoylation of the EGFR ligand Spitz by Rasp increases Spitz activity by restricting its diffusion, *Dev. Cell 10*, 167−176.
6. Drisdel, R. C., and Green, W. N. (2004) Labeling and quantifying sites of protein palmitoylation, *Biotechniques 36*, 276−285.
7. Roth, A. F., Wan, J., Bailey, A. O., Sun, B., Kuchar, J. A., Green, W. N., Phinney, B. S., Yates, J. R., and Davis, N. G. (2006) Global analysis of protein palmitoylation in yeast, *Cell 125*, 1003−1013.
8. Schlesinger, M. J., Magee, A. I., and Schmidt, M. F. (1980) Fatty acid acylation of proteins in cultured cell, *J. Biol. Chem. 255*, 10021−10024.
9. Hang, H. C., Geutjes, E. J., Grotenbreg, G., Pollington, A. M., Bijlmakers, M. J., and Ploegh, H. L. (2007) Chemical probes for the rapid detection of fatty-acylated proteins in mammalian cells, *J. Am. Chem. Soc. 129*, 2744−2745.
10. Kostiuk, M. A., Corvi, M. M., Keller, B. O., Plummer, G., Prescher, J. A., Hangauer, M. J., Bertozzi, C. R., Rajaiah, G., Falck, J. R., and Berthiaume, L. G. (2008) Identification of palmitoylated mitochondrial proteins using a bio-orthogonal azido-palmitate analogue, *FASEB J. 22*, 721−732.
11. Martin, D. D., Vilas, G. L., Prescher, J. A., Rajaiah, G., Falck, J. R., Bertozzi, C. R., and Berthiaume, L. G. (2008) Rapid detection, discovery, and identification of post-translationally myristoylated proteins during apoptosis using a bio-orthogonal azidomyristate analog, *FASEB J. 22*, 797−806.
12. Heal, W. P., Wickramasinghe, S. R., Bowyer, P. W., Holder, A. A., Smith, D. F., Leatherbarrow, R. J., and Tate, E. W. (2008) Site-specific N-terminal labelling of proteins *in vitro* and *in vivo* using N-myristoyl transferase and bioorthogonal ligation chemistry, *Chem. Commun. (Cambridge, U. K.)* 480−482.
13. Heal, W. P., Wickramasinghe, S. R., Leatherbarrow, R. J., and Tate, E. W. (2008) N-Myristoyl transferase-mediated protein labelling *in vivo*, *Org. Biomol. Chem. 6*, 2308−2315.
14. Hsu, T. L., Hanson, S. R., Kishikawa, K., Wang, S. K., Sawa, M., and Wong, C. H. (2007) Alkynyl sugar analogs for the labeling and visualization of glycoconjugates in cells, *Proc. Natl. Acad. Sci. U.S.A. 104*, 2614−2619.
15. Speers, A. E., Adam, G. C., and Cravatt, B. F. (2003) Activity-based protein profiling *in vivo* using a copper(I)-catalyzed azide-alkyne [3 + 2] cycloaddition, *J. Am. Chem. Soc. 125*, 4686−4687.
16. Speers, A. E., and Cravatt, B. F. (2004) Profiling enzyme activities *in vivo* using click chemistry methods, *Chem. Biol. 11*, 535−546.
17. Devadas, B., Lu, T., Katoh, A., Kishore, N. S., Wade, A. C., Mehta, P. P., Rudnick, D. A., Bryant, M. L., Adams, S. P., Li, Q., Gokelp, G. W., and Gordon, J. l. (1992) Substrate specificity of *Saccharomyces cerevisiae* myristoyl-CoA:protein N-myristoyltransferase. Analysis of fatty acid analogs containing carbonyl groups, nitrogen heteroatoms, and nitrogen heterocycles in an *in vitro* enzyme assay and subsequent identification of inhibitors of human immunodeficiency virus I replication, *J. Biol. Chem. 267*, 7224−7239.
18. Peseckis, S. M., Deichaite, I., and Resh, M. D. (1993) Iodinated fatty acids as probes for myristate processing and function. Incorporation into pp60v-src, *J. Biol. Chem. 268*, 5107−5114.
19. Brown, C. A., and Yamashita, A. (1975) Saline hydrides and superbases in organic reactions. IX. Acetylene zipper. Exceptionally facile contrathermodynamic multipositional isomerization of alkynes with potassium 3-aminopropylamide, *J. Am. Chem. Soc. 97*, 891−892.
20. Wang, Q., Chan, T. R., Hilgraf, R., Fokin, V. V., Sharpless, K. B., and Finn, M. G. (2003) Bioconjugation by copper(I)-catalyzed azide-alkyne [3 + 2] cycloaddition, *J. Am. Chem. Soc. 125*, 3192−3193.
21. Zornetzer, G. A., Fox, B. G., and Markley, J. L. (2006) Solution structures of spinach acyl carrier protein with decanoate and stearate, *Biochemistry 45*, 5217−5227.
22. Martin, B. R., and Cravatt, B. F. (2009) Large-scale profiling of protein palmitoylation in mammalian cells, *Nat. Methods 6*, 135−138.
23. Zha, J., Weiler, S., Oh, K. J., Wei, M. C., and Korsmeyer, S. J. (2000) Posttranslational N-myristoylation of BID as a molecular switch for targeting mitochondria and apoptosis, *Science 290*, 1761−1765.
24. Vilas, G. L., Corvi, M. M., Plummer, G. J., Seime, A. M., Lambkin, G. R., and Berthiaume, L. G. (2006) Posttranslational myristoylation of caspase-activated p21-activated protein kinase 2 (PAK2) potentiates late apoptotic events, *Proc. Natl. Acad. Sci. U.S.A. 103*, 6542−6547.
25. Charron, G., Zhang, M. M., Yount, J. S., Wilson, J., Raghavan, A. S., Shamir, E., and Hang, H. C. (2009) Robust fluorescent detection of protein fatty-acylation with chemical reporters, *J. Am. Chem. Soc. 131*, 4967−4975.